



**HAL**  
open science

## Satellite-based high latitude snow volume trend, variability and contribution to sea level over 1989/2006

Sylvain Biancamaria, Anny Cazenave, Nelly Mognard, W. Llovel, Frédéric  
Frappart

► **To cite this version:**

Sylvain Biancamaria, Anny Cazenave, Nelly Mognard, W. Llovel, Frédéric Frappart. Satellite-based high latitude snow volume trend, variability and contribution to sea level over 1989/2006. *Global and Planetary Change*, 2011, 75 (3-4), pp.99-107. 10.1016/j.gloplacha.2010.10.011 . hal-00575518

**HAL Id: hal-00575518**

**<https://hal.science/hal-00575518>**

Submitted on 10 Mar 2011

**HAL** is a multi-disciplinary open access archive for the deposit and dissemination of scientific research documents, whether they are published or not. The documents may come from teaching and research institutions in France or abroad, or from public or private research centers.

L'archive ouverte pluridisciplinaire **HAL**, est destinée au dépôt et à la diffusion de documents scientifiques de niveau recherche, publiés ou non, émanant des établissements d'enseignement et de recherche français ou étrangers, des laboratoires publics ou privés.

1 **Satellite-based high latitude snow volume trend, variability and**  
2 **contribution to sea level over 1989/2006**

3  
4 Sylvain Biancamaria <sup>1,2,3,\*</sup>, Anny Cazenave <sup>1,2</sup>, Nelly M. Mognard <sup>1,2</sup>, William Llovel <sup>1,3</sup>  
5 and Frédéric Frappart <sup>4</sup>

6  
7 <sup>1</sup> Université de Toulouse; UPS (OMP-PCA); LEGOS; 14 Av. Edouard Belin, F-31400  
8 Toulouse, France

9 <sup>2</sup> CNES; LEGOS, F-31400 Toulouse, France

10 <sup>3</sup> CNRS; LEGOS, F-31400 Toulouse, France

11 <sup>4</sup> Université de Toulouse; UPS (OMP-SVT); LMTG; 14 Av. Edouard Belin, F-31400  
12 Toulouse, France

13  
14  
15  
16  
17  
18  
19  
20  
21  
22  
23  
24 \* Corresponding author: [sylvain.biancamaria@legos.obs-mip.fr](mailto:sylvain.biancamaria@legos.obs-mip.fr) (Phone: +335 61 33 29 30;

25 Fax: +335 61 25 32 05)

26 Abstract

27

28 Snow volume change over the 1989/2006 period has been derived from Special Sensor  
29 Microwave/Imager (SSM/I) radiometric measurements for all land surfaces above 50°N,  
30 except Greenland. The mean annual snow volumes over the whole study domain, Eurasia and  
31 North America are respectively equal to 3713 km<sup>3</sup>, 2272 km<sup>3</sup> and 1441 km<sup>3</sup>, for the Pan  
32 Arctic regions, over this 18-year time period. While the snow volume exhibits a statistically  
33 significant negative trend ( $-9.7 \pm 3.8 \text{ km}^3 \cdot \text{year}^{-1}$ , p-value=0.02) over North America, it presents  
34 a positive, but not statistically significant trend ( $11.3 \pm 9.3 \text{ km}^3 \cdot \text{year}^{-1}$ , p-value=0.25) over  
35 Eurasia. These opposite variations can be related to different regional climatic conditions over  
36 these two regions: over Eurasia, snow depth is mainly influenced by the Arctic Oscillation  
37 (AO) and the Atlantic Multidecadal Oscillation (AMO) - correlation coefficient = 0.68  
38 between the SSM/I-derived snow volume and a linear combination of AO and AMO indices,  
39 whereas over North America snow depth is mainly influenced by the Pacific North American  
40 (PNA) pattern and the AMO - correlation coefficient = 0.75 for a linear combination of the  
41 PNA and AMO indices. This study confirms that snow volume is a key driver of the sea level  
42 seasonal cycle, but net snow volume trend for the Pan Arctic regions indicates a negligible  
43 and not statistically significant contribution to sea level rise ( $-0.004 \pm 0.009 \text{ mm} \cdot \text{year}^{-1}$ , p-  
44 value=0.88 once converted into sea level).

45

46 Keywords: SSM/I; snow volume; high latitude; climate indices; sea level

47

## 48 1. Introduction

49

50 High latitude regions are the most affected by current climate change (e. g. Trenberth  
51 et al., 2007). Different components of the Arctic hydrological cycle have experienced  
52 important modifications since the beginning of the 20<sup>th</sup> century. For example river discharge  
53 has significantly increased (Stocker and Raible, 2005), snow extent is decreasing (Déry and  
54 Brown, 2007; Brown et al., 2010) and the annual duration of the period with unfrozen soil  
55 conditions has increased (Groisman et al., 2006). Snow volume is a key variable to understand  
56 the evolution of the high latitude hydrological cycle. High latitude rivers discharge is mainly  
57 driven by the accumulated snow volume and the timing of its melting, leading to extremely  
58 important floods in spring (Yang et al., 2003). So, snow cover extent and depth are among the  
59 Essential Climate Variables (ECV) of the Global Climate Observing System (GCOS; Sessa  
60 and Dolman, 2008) and observations of their temporal evolution are of critical importance.  
61 Few *in situ* snow observations are available at high latitude, thus providing limited  
62 information on global and regional snow depth fields (Brown, 2000). Remote sensing  
63 techniques complement the *in situ* data, but most analyses focused on snow extent change (see  
64 Trenberth et al., 2007 for a review), which only partially characterize snow variability. So far,  
65 interannual to multidecadal changes in snow volume have been mainly estimated using  
66 hydrological model outputs (e.g. Milly et al., 2003). In this study, we use satellite-based  
67 microwave observations to derive and analyze high latitude snow volume changes over  
68 1989/2006. Correlations between snow volume and climate indices have been investigated  
69 and the Arctic snow contribution to the global mean sea level variation has been estimated.

70

## 71 2. Data analysis

72

73           Snow volume used in this study has been computed from Special Sensor  
74 Microwave/Imager (SSM/I) data. SSM/I measures the Earth brightness temperature for  
75 different microwave frequencies in both horizontal and vertical polarizations (19.35 GHz, 37  
76 GHz, 85.5 GHz and 22.235 GHz). Since July 1987, this instrument has been operating on  
77 board the operational Defense Meteorological Satellite Program satellite series. Daily SSM/I  
78 data, mapped to the Equal Area SSM/I Earth Grid projection with a 25×25 km<sup>2</sup> resolution, are  
79 provided by the National Snow and Ice Data Center (Armstrong et al., 1994). A dynamic  
80 algorithm that takes into account the temporal evolution of the snow grain size, developed by  
81 Mognard and Josberger (2002), has been used to retrieve snow depth from SSM/I  
82 measurements. This algorithm has been first developed for the U.S. Northern Great Plains,  
83 then amended by Grippa et al. (2004) and applied over Western Siberia. Recently, a multi-  
84 year (1988/1995) averaged snow depth field computed using this algorithm has been validated  
85 over Siberia (Boone et al., 2006) and the whole high latitude regions, Greenland excluded  
86 (Biancamaria et al., 2008). Interannual variability of these data has been validated over the Ob  
87 river basin, in Western Siberia, by comparison with discharge measurements at the estuary  
88 (Grippa et al., 2005). The latter study found a significant correlation between the snowmelt  
89 date and the discharge in May (correlation coefficient = -0.92) and between the winter snow  
90 depth and the discharge in June (correlation coefficient = 0.61).

91           The inputs for this algorithm are the difference between 19.35 GHz and 37 GHz  
92 brightness temperature in horizontal polarization from SSM/I, the air/snow interface  
93 temperatures from the National Centers for Environmental Prediction global (NCEP)  
94 reanalysis (Kalnay et al., 1996) and the snow/ground interface temperatures modeled by the  
95 “Interaction between Soil-Biosphere-Atmosphere” (ISBA) scheme forced by the Global Soil  
96 Wetness Project-Phase2 P3 precipitation field (Boone et al., 2006). For the present study, we  
97 consider all continental surfaces above 50°N, Greenland excluded, composed of two sub-

98 regions: Eurasia ( $0^{\circ}\text{E}<\text{longitude}<191^{\circ}\text{E}$ ) and North America ( $191^{\circ}\text{E}<\text{longitude}<360^{\circ}\text{E}$ ).  
99 Regions below  $50^{\circ}\text{N}$  have not been taken into account as the snowpack is highly variable  
100 spatially and of low amplitude, hence difficult to observe with a  $25\times 25\text{ km}^2$  spatial resolution.  
101 According to the snow climatology over North America from Brown et al. (2003), between  
102 December and March, 80% of the total North American snow volume is found above  $50^{\circ}\text{N}$ .

103 This study focuses on monthly and yearly-averaged total snow volume (sum of all  
104 non-zero snow depth pixels multiplied by the pixel area). Yearly averages are centered on  
105 winter months (i.e. the yearly average for year  $n$  corresponds to the temporal average from  
106 October year  $n-1$  to September year  $n$ ).

107 Snow volume derived from SSM/I measurements for January, and temporally  
108 averaged over 1989/2006, has been compared to the 1979/1996 climatology for North  
109 America from Brown et al. (2003) and to the global climatology from U.S. Air  
110 Force/Environmental Technical Applications Center (USAF/ETAC) (Foster and Davy, 1988).  
111 The correlation coefficient between snow depth from SSM/I and Brown et al. (2003) is 0.36.  
112 However most of the differences between the two datasets are found over regions covered  
113 with tundra, according to the snow classification from Liston and Sturm, 1998). For tundra-  
114 covered regions (42% of North America), the correlation coefficient is equal to 0.20, whereas  
115 over the remaining of North America the correlation coefficient is equal to 0.60 (the tundra  
116 covers 42% of North America). This result is consistent with the previous study by  
117 Biancamaria et al. (2008), which found that the dynamic algorithm does not perform well  
118 over the Northern part of the continent (where the tundra is located) due to the presence of  
119 numerous lakes. The SSM/I data over these regions need to be processed using a specific  
120 algorithm, such as the one developed by Derksen et al. (2010), to take into account the  
121 specificity of snow emissivity over lakes. Yet, this still remains an open issue, which requires  
122 further investigations since, the *in situ* snow gauges, used by Brown et al. (2003) to compute a

123 climatology by interpolation are very scarce above 50°N, especially for the Northern part of  
124 the continent. snow depth from SSM/I correlates better with the USAF/ETAC climatology  
125 (correlation coefficient equals to 0.62 over the whole study domain, 0.67 over Eurasia and  
126 0.52 over North America ), These correlation coefficients are highly significant, as their p-  
127 values (i.e. the probability to obtain these coefficients by random chance, whereas the  
128 variables are uncorrelated) are extremely small (lower than 0.001). The snow depth retrieved  
129 from SSM/I measurements are not directly compared to *in situ* measurements as the spatial  
130 resolution of SSM/I is too coarse to be compared to local measurements, and high latitude  
131 networks of *in situ* snow depth measurements are not dense enough to allow an estimation of  
132 the mean snow depth over a 25x25 km<sup>2</sup> area. Based on a statistical analysis over the U.S.  
133 Northern Great Plains, Chang et al. (2005) showed that error between one single *in situ*  
134 measurement and the mean snow depth over a 1°x1° region can be up to 20 cm (for a range of  
135 snow depth values between 1.5 cm and 45.4 cm).

136         The temporal variability of the SSM/I-derived snow volume is analyzed in the next  
137 section. It agrees well with previous published studies, giving high confidence in the quality  
138 of the snow volume time series estimated from SSM/I observations.

139

### 140 3. Snow volume temporal variability

141

142 Figure 1 shows the monthly anomalies of snow volume time series averaged over the study  
143 area from SSM/I, from an inversion of the Level-2 GFZ Gravity Recovery And Climate  
144 Experiment (GRACE) products (Ramillien et al., 2005; Frappart et al., 2006), from the  
145 European Centre for Medium-Range Weather Forecasts ReAnalysis (ERA)-interim product  
146 (Uppala et al., 2008), and outputs from two Land Surface Models (LSM) used by the Global  
147 Land Data Assimilation System (GLDAS) (Rodell et al., 2004): MOSAIC (Koster and

148 Suarez, 1996) and NOAA 2.7 (Chen et al., 1996), between January 2003 and June 2006. The  
149 mass variations measured by GRACE have been converted into snow volume assuming a  
150 constant snow volume density of  $300 \text{ kg.m}^{-3}$ . The time variations of the snow volume are  
151 dominated by the seasonal cycle. NOAA outputs present a better agreement with GRACE  
152 data both in terms of amplitude and timing. Snow volume from SSM/I is in better agreement  
153 with MOSAIC for the amplitude and with ERA-interim for the phase. However, all datasets  
154 agree well in phase and their amplitudes have the same order of magnitude, except for ERA-  
155 interim which seems to overestimate the amplitude. The GRACE land water and snow  
156 solutions used in this study, are based on the development of geopotential harmonic  
157 coefficients up to a degree 50, which correspond to a spatial resolution of 400 km (see  
158 Frappart et al. (in press) for more details about this dataset). This leads to smaller amplitudes  
159 and smoothes the temporal time series. Table 1 presents the annual snow volume trends over  
160 2003/2006 computed from SSM/I-based snow depth, from the snow reservoir extracted from  
161 GRACE measurements and from the total GRACE signal over the whole study domain,  
162 Eurasia and North America. Two trends computed from GRACE data are shown: the first one  
163 has been directly computed from the GRACE (snow and total) time series and the second one  
164 has been corrected from the Post-Glacial Rebound (PGR) trend estimated by Paulson et al.  
165 (2007), available on the GRACE Tellus website (<http://grace.jpl.nasa.gov>). The uncertainties  
166 on PGR trends are supposed to be around 20% (Paulson et al., 2007) and are given in  
167  $\text{mm.year}^{-1}$  of equivalent water thickness, which have been converted into snow volume trends  
168 using a constant snow density of  $300 \text{ kg.m}^{-3}$ . The PGR trend (in equivalent snow volume per  
169 year) is equal to  $495.6 \text{ km}^3.\text{year}^{-1}$ ,  $31.2 \text{ km}^3.\text{year}^{-1}$  and  $464.4 \text{ km}^3.\text{year}^{-1}$  over the whole study  
170 domain, Eurasia and North America, respectively. SSM/I and PGR corrected GRACE trends  
171 are all negative, as previously observed at basin-scale for the GRACE data by Frappart et al.  
172 (in press), yet they are statistically significant only over North America. The differences



173 between SSM/I and GRACE trends are likely caused by the sensitivity due to the small  
174 number of years available for the computation, the truncation of the GRACE data (which  
175 caused a loss of energy in the short spatial wavelengths) and PGR uncertainty.

176 Interannual total snow volume time series (seasonal signal removed) from SSM/I has  
177 been computed over 1989/2006 for the whole study domain (Figure 2a) and separately for  
178 Eurasia (Figure 2b) and for North America (Figure 2c). Table 2 presents the mean, standard  
179 deviation and trend (with the p-value) of the SSM/I-based snow volume over 1989/2006.  
180 ERA-interim data has not been used because of biases in the background forecast and in the  
181 assimilated observations that makes them unreliable for trend estimation (Trenberth et al.,  
182 2007). Even if an effort has been undertaken to reduce the biases in ERA-interim (Dee and  
183 Uppala, 2009), trends computed with this dataset should still be used with caution. Outputs  
184 from GLDAS are not shown, due to the presence of an obvious bias in these datasets between  
185 the 1989/1999 and 2000/2006 time periods. For NOAH, the mean snow volume and standard  
186 deviation over 1989/1999 are equal to  $6239 \text{ km}^3$  and  $329 \text{ km}^3$ , respectively, whereas over  
187 2000/2006 they are equal to  $4760 \text{ km}^3$  and  $183 \text{ km}^3$ , respectively. Thus, trends computed from  
188 these snow depth fields will mainly be the result of this bias.

189 SSM/I snow volume over Eurasia displays a positive, but not statistically significant,  
190 trend of  $11.3 \pm 9.3 \text{ km}^3 \cdot \text{year}^{-1}$  (p-value=0.25, Figure 2b), while over North America the trend is  
191 negative and statistically significant ( $-9.7 \pm 3.8 \text{ km}^3 \cdot \text{year}^{-1}$ , p-value=0.02, Figure 2c). Trends  
192 have been computed using the generalized linear model regression (Dobson, 1990), and the  
193 uncertainty given with each trend corresponds to the standard error on the estimation of the  
194 slope from the linear regression algorithm used. These uncertainties are high as snow volume  
195 time series have large variability. When the yearly snow volume is averaged over the whole  
196 study domain, the trend is positive, remains small, with a very large uncertainty and is not  
197 statistically significant ( $1.5 \pm 10.5 \text{ km}^3 \cdot \text{year}^{-1}$ , p-value=0.88, Figure 2a). Figure 3 presents the

198 regional distribution of snow depth trends over 1989/2006 (only statistically significant  
199 trends, i.e.  $p\text{-value} < 0.1$ , are shown). Over Eurasia, the highest positive trends are found over  
200 the Lena basin, the southern part of the Yenisey basin (between  $60^{\circ}\text{N}/70^{\circ}\text{N}$  and  $100^{\circ}\text{E}/130^{\circ}\text{E}$ )  
201 and Eastern Europe. Over North America, Quebec, Baffin Island and the Arctic Ocean coast  
202 show negative trends, whereas positive trends are found over the Rockies and Southern  
203 Alaska. Previous studies interpolated sparse *in situ* measurements to infer temporal evolution  
204 of snow cover. Groisman et al. (2006) analyzed 1811 *in situ* observations of the soil condition  
205 (classified as frozen or unfrozen) between 1956 and 2004, within  $1197\ 1^{\circ}\times 1^{\circ}$  grid cells over  
206 the former Soviet Union (most of these grid cells containing only one *in situ* station). The *in*  
207 *situ* network used is very sparse above  $55^{\circ}\text{N}$  and East of the Ural Mountains. Groisman et al.  
208 (2006) observed a significant increase in the number of days with unfrozen soil conditions  
209 between 1956 and 2004. Yet, this increase is most frequently due to a reduction of days with  
210 frost and ice on the ground rather than a snow cover retreat. Besides, these modifications tend  
211 to diminish during the last decade of the twentieth century. These observations agree with our  
212 results (a positive, but not significant, snow volume trend over Eurasia). Bulygina et al.  
213 (2009) used 820 *in situ* stations over Russia between 1966 and 2007 to infer snow depth trend  
214 maps. They found that snow cover periods tend to be shorter, however the amount of snow  
215 fall tends to increase, leading to positive snow depth trends over Eurasia: maximum storage  
216 change increased from  $0.2\ \text{cm}\cdot\text{year}^{-1}$  to  $0.6/0.8\ \text{cm}\cdot\text{year}^{-1}$  (with maximum rates in Western  
217 Siberia). These trends have the same order of magnitude than trends shown in Figure 3. Based  
218 on *in situ* measurements, Kitaev et al. (2005) found a positive snow depth trend ( $0.09\ \text{cm}\cdot\text{year}^{-1}$ )  
219 over Eurasia (for latitudes above  $40^{\circ}\text{N}$ ) for February between 1936/2000. This study also  
220 showed opposite trends between snow water equivalent in February for 1966/2000 over  
221 Eurasia and North America (the trends are equal to  $0.743\ \text{mm}/\text{decade}$  and  $-1.231\ 743$   
222  $\text{mm}/\text{decade}$ , respectively). For February of the 1989/2006 time span, SSM/I-based snow depth

223 trends are equal to  $0.14 \text{ cm}\cdot\text{year}^{-1}$  (p-value=0.15) over Eurasia and  $-0.18 \text{ cm}\cdot\text{year}^{-1}$  (p-  
224 value=0.02) over North America. These results are in agreement with the results found by  
225 Kitaev et al. (2005).

226 Using different data sets (visible and microwave satellite observations, objective  
227 analyses of surface snow depth observations, reconstructed snow cover from daily  
228 temperature and precipitation, and proxy information derived from thaw dates), Brown et al.  
229 (2010) showed that snow cover extent in June and May respectively decreased by 46% and a  
230 14% in the Arctic (latitude>60°N), during the 1967/2008 time period. This reduction is  
231 observed over both Eurasia and North America and 56% of snow cover extent variability for  
232 June and 49% for May is explained by air temperature. Using a less accurate data set, Déry  
233 and Brown (2007) showed that snow cover extent also decreased in Eurasia and North  
234 America during winter time for the 1972/2006 time span. However, the observed decline is  
235 smaller than during spring. The snow volume variability computed in our study does not seem  
236 to be consistent with the trend in snow cover extent observed in these previous studies,  
237 especially over Eurasia. Yet, this was expected. In effect, Ge and Gong (2008) showed that, at  
238 continental/regional scales, high latitude snow extent and snow depth are largely unrelated.

239 The decreasing trend of snow volume over North America estimated from SSM/I is in  
240 agreement with the previous study from Dyer and Mote (2006). Using interpolated *in situ*  
241 measurements during the 1960/2000 time span, they found that snow depth has a decreasing  
242 trend in January/February over the time period, which becomes even steeper around March,  
243 along with an earlier onset of spring thaw, which could explain the decreasing North  
244 American snow volume trend observed in our study.

245 It is extremely difficult to estimate the implications of the observed decreased in North  
246 American snow volume on other snow related parameters, like glaciers mass, and an answer  
247 to this issue is far beyond the scope of this paper. For example, very recently, Berthier et al.

248 (2010) confirmed that Alaskan glaciers are losing mass. However, glaciers mass loss is not  
249 only observed in North America, but is widely measured on all continents (Kaser et al., 2006).  
250 Therefore, it is hard to assess if there is any relation between the Alaskan glaciers mass loss  
251 and the decreasing snow volume in North America, and this issue will require further  
252 investigations.

253

#### 254 4. Relationship between snow volume and climate indices

255

256 To investigate the causes of snow volume variability in North America and Eurasia,  
257 yearly mean SSM/I snow volume anomaly has been correlated to climate indices representing  
258 the dominant modes of atmospheric and ocean variability. The following climate indices have  
259 been considered:

260 - Arctic Oscillation (AO, leading mode from the Empirical Orthogonal Function analysis of  
261 monthly mean height anomalies at 1000-hPa, poleward of 20°N). A positive (negative) AO  
262 index corresponds to a lower (higher) than normal atmospheric pressure over the Arctic,  
263 which leads to stronger (weaker) westerly winds. Therefore, in positive AO phase, cold  
264 Arctic air is maintained in the Northern part of America (Arctic coast and Quebec), while the  
265 rest of America, Europe and Asia experiences a warmer than averaged winter, with more  
266 precipitation in Northern Europe. On the contrary, in negative AO phase, cold Arctic air  
267 reaches lower latitude (South Canada, US, Asia and Europe), whereas the Northern parts of  
268 America is warmer than during the positive AO phase (Thompson and Wallace, 1998).

269 - Atlantic Multidecadal Oscillation (AMO, North Atlantic mean sea surface temperature  
270 anomaly north of the equator). AMO corresponds to cycles of warming and cooling of the  
271 North Atlantic Ocean with a period comprised between 50 and 80 years. This cycle affects the  
272 North Atlantic branch of the thermohaline circulation and therefore the whole oceanic system

273 (Kerr, 2000). A positive (negative) phase of the AMO leads to more (less) summer  
274 precipitations in Northern Europe and Alaska and less (more) summer precipitations in the  
275 U.S. and South Canada (Enfield et al., 2001). Knight et al. (2006) show, using a climate  
276 model, that positive AMO phase tends to strengthen broad cyclonic pressure anomalies over  
277 the Atlantic and Europe in winter, therefore increasing precipitations on these regions. During  
278 the time span of the study (1989/2006), the AMO has shifted from a negative to a positive  
279 phase around 1995.

280 - Pacific Decadal Oscillation (PDO, leading principal component of monthly sea surface  
281 temperatures in the North Pacific, poleward of 20°N). PDO is an El Niño-like pattern  
282 characteristic the North Pacific climate variability with interannual to interdecadal  
283 fluctuations. PDO influences mainly North America climate during winter time and is  
284 positively correlated with precipitation along the coasts and central Gulf of Alaska and  
285 negatively correlated over much of the interior of North America (Mantua et al., 1997).

286 - Pacific North American pattern (PNA, second component of the Northern Hemisphere extra  
287 tropical sea level pressure anomalies). During positive (negative) phase of the PNA,  
288 geopotential height anomalies are positive (negative) along the West coast of North America  
289 and negative (positive) in the mid-Pacific and Eastern US. Therefore, negative PNA phase is  
290 characterized by a strong East Asian jet stream, which is blocked during positive PNA phase.  
291 The spatial scale of the PNA pattern is at its most extent during winter (Wallace and Gutzler,  
292 1981).

293 Data have been computed by the National Oceanic and Atmospheric Administration  
294 (NOAA)/Climate Prediction Center (CPC), the NOAA/Earth System Research Laboratory  
295 (ESRL) and the Joint Institute for the Study of the Atmosphere and Ocean (JISAO)/University  
296 of Washington (UW), and have been downloaded from

297 [http://ioc3.unesco.org/oopc/state\\_of\\_the\\_ocean/atm](http://ioc3.unesco.org/oopc/state_of_the_ocean/atm). Each index has been averaged from  
298 January through March for each year.

299 Figure 4 presents annual snow volume time series over Eurasia and North America  
300 along with the January to March average of the climate indices presented above. As snow  
301 volumes and the indices do not have the same units and range of variations, all time series  
302 shown in Figure 4 have been normalized and centered. On each plot, the gray horizontal line  
303 corresponds to the zero in the original climate index time series. Table 3 gives the correlation  
304 coefficients between the climate indices and the annual snow volumes over North America  
305 and Eurasia. The AO index is relatively well correlated with snow volume over North  
306 America (correlation=0.51 and p-value=0.03, Figure 4b) and anti-correlated with snow  
307 volume over Eurasia (correlation=-0.57 and p-value=0.01, Figure 4a), thus the climatic  
308 conditions represented by the AO index (which is the dominant mode of interannual  
309 variability in North Hemisphere) play a significant and opposite role over the two continents.  
310 It is worth mentioning that SSM/I snow volume over Eurasia and North America are not  
311 correlated (correlation=-0.07 and p-value=0.80). AMO and PNA are anti-correlated with  
312 snow volume over North America (correlation=-0.59 with p-value=0.01 and correlation=-0.66  
313 with p-value=0.003, respectively) and not, or only weakly, correlated with snow volume over  
314 Eurasia (correlation=0.04 with p-value=0.88 and correlation=0.30 with p-value=0.22,  
315 respectively). On the contrary, PDO is more strongly linked with snow volume over Eurasia  
316 (correlation=0.49 with p-value=0.04) than over North America (correlation=-0.18 with p-  
317 value=0.47). Figure 5 presents snow depth linear regression maps based on each climate  
318 index (i.e. the correlation coefficient between snow depth and the climate index multiplied by  
319 the snow depth standard deviation for each pixel), which clearly show the locations where  
320 snow depth co-varies with each climate index. On these maps, regression coefficients are  
321 presented only for pixels which have a statistically significant (p-value<0.1) correlation

322 coefficient. Regression map between snow depth and AO index (Figure 5a) clearly shows the  
323 opposite impact of AO index over snow depth between North American Arctic coast and the  
324 Eastern part of Siberia (with positive regression coefficients) and middle Siberia and Eastern  
325 Europe (with negative regression coefficients). There are few statistically significant  
326 regression coefficients between snow depth and AMO index over Eurasia (Figure 5b), some  
327 negative regression coefficients over Quebec and North American Arctic coast and some  
328 positive coefficients over the Rockies. Snow depth weakly co-varies with PDO index over  
329 North America (Figure 5c), contrarily to Southern middle Siberia and Northeastern Europe,  
330 where regression coefficients are positive. Finally, regression coefficients between snow  
331 depth and PNA index (Figure 5d) show that PNA is linked with snow depth especially in  
332 central North America (negative coefficients), in the Rockies (positive coefficients) and in  
333 Southern middle Siberia (positive coefficients). From these results, it seems that AO is the  
334 only mode affecting significantly snow volumes over both Eurasia and North America and  
335 could explain the different behavior of snow volume over these two continents.

336 Previous studies (Cohen et al., 2007; Orsolini and Kvamstø, 2009) have shown that  
337 high snow cover in late autumn over Eurasia can create upward propagating planetary wave  
338 pulses in winter, which weaken the polar vortex and therefore lead to negative AO in late  
339 winter, explaining a negative correlation between snow cover extent and AO index. The same  
340 process also explains the negative correlation between snow volume over Eurasia and winter  
341 AO index observed in our study.

342 Ge and Gong (2009) compared monthly AO, NAO (North Atlantic Oscillation,  
343 commonly seen as a regional manifestation of AO), PDO and PNA indices with monthly *in*  
344 *situ* interpolated snow depth over North America during the 1956/2000 time span. They found  
345 that snow depth has weak correlation with monthly AO and NAO indices, but strong anti-  
346 correlation with monthly PDO and PNA indices for the winter months (December to April).

347 However, for PDO, only correlation coefficients for February and March are significant at  
348 90% confidence level (for PNA all the correlations during all winter months are above the  
349 90% confidence level). Our results seem to differ partially, as we found that snow volume  
350 significantly correlates with AO, significantly anti-correlates with PNA and has no significant  
351 linear relationship with PDO over North America. However, it should be noted that Ge and  
352 Gong (2009) studied a wider domain (with latitudes below 35°N) and found the highest  
353 relations between snow depth and PDO/PNA over interior central-western North America,  
354 which expands far below 50°N (the Southern limit of our study domain). Ghatak et al. (2010)  
355 used the same North American *in situ*-based snow depth field than Ge and Gong (2009) and  
356 found that globally snow depths correlate negatively with both winter NAO and PNA. Yet,  
357 their study domain includes the whole North American continent. If only the latitudes above  
358 50°N are considered (Figure 4 and 6 in Ghatak et al., 2010), they showed that snow depth  
359 correlates positively with NAO and negatively with PNA, as found in our study (Table 3).  
360 Their explanation of these correlations is the following: positive phase of winter NAO leads  
361 to higher air temperature anomalies over eastern North America, reducing snow volume;  
362 positive phase of the winter PNA leads to stronger East Asian jet stream and thus more  
363 snowfall in Northwest America but to less snowfall in Northeast America and near the Arctic  
364 coast (which is in agreement with the regression map between snow depth and PNA, Figure  
365 5d).

366 To better examine inter-annual co-variability between snow volume and climate  
367 indices, the linear trend in all time series has been removed and the corresponding correlation  
368 coefficients have been computed (Table 3). Over Eurasia, the most statistically significant  
369 correlations are still obtained with the AO (correlation=-0.51 with p-value=0.03) and PDO  
370 (correlation=0.41 with p-value=0.09) indices. Over North America, the only statistically  
371 significant correlation is obtained with PNA index (correlation=-0.58 with p-value=0.01),



372 which means that North American snow volume linear trend could be related to the AO and  
373 AMO indices (probably due to the shift from a negative to a positive AMO around 1995),  
374 whereas snow volume inter-annual variability is more linked with the PNA pattern.

375         The correlation coefficients between yearly mean snow volume anomaly and all  
376 possible linear combinations of two different climate indices have also been computed. For  
377 Eurasia, the best correlation coefficient (0.68, p-value=0.002) is obtained for a linear  
378 combination between AO and AMO (-156.AO-611.AMO, blue curve in Figure 2b), whereas  
379 for North America the best correlation coefficient (0.75, p-value<0.01) is obtained for a linear  
380 combination between PNA and AMO (-235.AMO-92.PNA, blue curve in Figure 2c). AO and  
381 PNA, when combined with AMO, influence respectively the most Eurasia and North America  
382 snow volume and represent regional atmospheric processes influencing the two continents. If  
383 the trend is removed from both climate indices and snow volume, the best correlation  
384 coefficient is still obtained with a linear combination of AO and AMO indices over Eurasia (-  
385 136.AO-940.AMO, correlation=0.68 and p-value=0.002). Surprisingly, linear combination of  
386 AO and PDO indices, which individually gives respectively the first (-0.51) and second (0.41)  
387 best correlations with snow volume over Eurasia, only corresponds to the second best  
388 correlation between a linear combination of two climate indices and snow volume (-  
389 96.AO+76.PDO, correlation=0.58 and p-value=0.01). Over North America, the best  
390 correlation is obtained with a linear combination of PDO and PNA indices (37.PDO-  
391 114.PNA, correlation=0.66 and p-value=0.003), however the second best correlation is  
392 obtained with AMO and PNA indices (-165.AMO-87.PNA, correlation=0.61 and p-  
393 value=0.007).

394

395 5. Snow and sea level

396

397 High latitude snow has a large impact on river discharge and thus is the main source of  
398 fresh water input to the Arctic Ocean. Snow volume change ( $V_{snow}$ ) presented in the previous  
399 sections can be used to estimate the snow contribution to the global mean sea level ( $SLV_{snow}$ ),  
400 using equation (1).

401

$$402 \quad SLV_{snow} = -\frac{\rho_{snow}}{\rho_{water} \cdot A_{ocean}} \cdot V_{snow} \quad (1)$$

403

404 where  $\rho_{snow}=300 \text{ kg.m}^{-3}$  (snow density),  $\rho_{water}=1000 \text{ kg.m}^{-3}$  (liquid water density) and  
405  $A_{ocean}=3.6 \times 10^8 \text{ km}^2$  (total oceanic domain).

406 Over 1989/2006, the snow volume trend from SSM/I converted into equivalent sea  
407 level is very small ( $-0.0013 \pm 0.0087 \text{ mm.yr}^{-1}$ ) and not statistically significant. The snow  
408 volume trend over the altimetry time span (1993/2006) amounts to  $-17.0 \pm 15.1 \text{ km}^3 \cdot \text{year}^{-1}$  (p-  
409 value=0.28), which yield small positive contributions to sea level of  $0.014 \pm 0.013 \text{ mm.yr}^{-1}$ . As  
410 this trend is not statistically significant and is negligible compared to the global mean sea  
411 level trend (of  $3.3 \pm 0.4 \text{ mm.yr}^{-1}$  over the satellite altimetry period 1993/2009; Cazenave and  
412 Llovel, 2010), it is obvious that high latitude snow does not play any role in the global mean  
413 sea level rise observed from satellite altimetry.

414 However, Arctic snow is a key component of the mean sea level seasonal cycle. To  
415 investigate this relationship, snow volume change has been compared to global mean sea level  
416 time series over 2002/2006 from Topex/Poseidon and Jason 1 computed by Collecte  
417 Localisation Satellite (CLS), available on the AVISO website ([www.aviso.oceanobs.com](http://www.aviso.oceanobs.com)).  
418 The mean sea level data have been corrected for steric effects (mainly thermal expansion of  
419 ocean waters) using the methodology developed by Llovel et al. (2010) and based on Argo  
420 data (Guinehut et al., 2009). Mean and trend have been removed from this corrected sea level  
421 and the seasonal cycle (i.e. the sinusoid with a 365.25 day period which best fits the time

422 series) has been least square adjusted. The sea level seasonal cycle has a maximum amplitude  
423 of 6.2 mm which occurs around 15 October. Snow volume converted into sea level (mean and  
424 trend removed) has a seasonal cycle with 4.1 mm maximum amplitude around 10 August. Its  
425 amplitude is smaller, but has the same order of magnitude than the global mean sea level  
426 seasonal cycle, yet breaks earlier. This phase lag could be due to the time taken by water from  
427 snow melt to be routed to the ocean by the river network. It could also be explained if water  
428 stored in other reservoirs like ground water and water vapor in the atmosphere is taken into  
429 account. To test this hypothesis, the seasonal cycle of the ground water has been  
430 approximated by a sinusoid with amplitude of 3 mm (in sea level equivalent) and a yearly  
431 maximum at the beginning of September (Cazenave et al., 2000). Similarly, the atmospheric  
432 water vapor has been approximated by a sinusoid with amplitude of 2 mm and a yearly  
433 maximum at the beginning of December (Cazenave et al., 2000). The sum of these three  
434 contributors (snow, ground water and water vapor) has an amplitude equal to 6.9 mm, which  
435 is very close to the global mean sea level seasonal cycle amplitude with a reduced phase lag  
436 (the maximum is around mid-September). This is a surprisingly good result given the large  
437 approximation used and clearly shows that Arctic snow variability is one of the main  
438 contributors to the global mean sea level seasonal cycle, as previously shown from model  
439 outputs by Chen et al. (1998), Minster et al. (1999), Cazenave et al. (2000) and Milly et al.  
440 (2003).

441

## 442 6. Conclusions and perspectives

443

444 From passive microwave data acquired between 1989 and 2006, it has been possible to  
445 estimate the high latitude snow volume variability. Over Eurasia, the mean annual snow  
446 volume trend is positive ( $11.3 \pm 9.3 \text{ km}^3 \cdot \text{year}^{-1}$ ), yet not statistically significant. Over North

447 America the snow volume trend is equal to  $-9.7 \pm 3.8 \text{ km}^3 \cdot \text{year}^{-1}$  and is statistically significant.  
448 This difference between the two continents could be due to AO which correlates with North  
449 American snow volume (correlation = 0.51) and anti-correlates with Eurasian snow volume  
450 (correlation = -0.57). These differences are also linked with regional climatic conditions as  
451 snow volume anomaly over North America better (anti-)correlates with the PNA index  
452 (correlation=-0.66), and AMO index (correlation=-0.59). However, the correlation between  
453 AMO and North American snow volume is mainly due to the trend and not to the interannual  
454 variability. Moreover, snow volume over Eurasia correlates well with a linear combination of  
455 the AO and AMO indices (correlation = 0.68), whereas over North America it correlates with  
456 a linear combination of the PNA and AMO indices (correlation = 0.75).

457 Finally, this study shows that high latitude snow volume does not contribute to the  
458 global mean sea level trend observed by satellite altimetry, but is a main component of the  
459 global mean sea level seasonal cycle.

460 In the future, it will be interesting to compare the snow volume trends observed in this  
461 study and trends from other hydrologic parameters in order to better understand the  
462 interaction between snow and the whole North Hemisphere high latitude hydrological cycle.

463

#### 464 Acknowledgments

465 The NSIDC is greatly thanked for processing and freely distributing SSM/I data.

466 The GLDAS data used in this study were acquired as part of the mission of NASA's Earth  
467 Science Division and archived and distributed by the Goddard Earth Sciences (GES) Data and  
468 Information Services Center (DISC). The Authors are thankful to J.-P. Vergnes for  
469 downloading and post-processing GLDAS data.

470 ECMWF ERA-Interim data used in this study have been obtained from the ECMWF data  
471 server.

472 The NOAA/CPC, NOAA/ESRL and JISAO/UW are acknowledged for letting the time series  
473 of the climate indices used in this study freely available to the community.  
474 The authors are particularly grateful to two anonymous reviewers for their constructive  
475 comments and suggestions, which significantly improved the quality of the manuscript.  
476 Three of the authors are supported by a CNES/Noveltis PhD grant (S. Biancamaria), a STAE  
477 foundation grant in the framework of the CYMENT project (F. Frappart) and a CNRS/Région  
478 Midi-Pyrénées PhD grant (W. Llovel).

479 References

480

481 Armstrong, R.L., Knowles, K.W., Brodzik, M.J., Hardman, M.A., 1994 (updated 2007).

482 DMSP SSM/I Pathfinder daily EASE-Grid brightness temperatures 1988-2006. National  
483 Snow and Ice Data Center, Digital media, Boulder, Colorado USA.

484

485 Berthier, E., Schiefer, E., Clarke, G.K.C., Menounos, B., Rémy, F., 2010. Contribution of  
486 Alaskan glaciers to sea-level rise derived from satellite imagery. *Nat. Geosci.*, 3, 92-95.

487

488 Biancamaria, S., Mognard, N.M., Boone, A., Grippa, M., Josberger, E.G., 2008. A satellite  
489 snow depth multi-year average derived from SSM/I for the high latitude regions. *Remote  
490 Sens. Environ.*, 112, 2557-2568.

491

492 Boone, A., Mognard, N.M., Decharme, B., Douville, H., Grippa, M., Kerrigan, K., 2006. The  
493 impact of simulated soil temperatures on the estimation of snow depth over Siberia from  
494 SSM/I compared to a multi-model multi-year average. *Remote Sens. Environ.*, 101, 482-494.

495

496 Brown, R.D., 2000. Northern Hemisphere snow cover variability and change, 1915-97. *J.  
497 Clim.*, 13, 2339-2355.

498

499 Brown, R.D., Brasnett, B., Robinson, D., 2003. Gridded North American monthly snow depth  
500 and snow water equivalent for GCM evaluation. *Atmos. Ocean.*, 41, 1-14.

501

502 Brown, R.D., Derksen, C., Wang, L., 2010. A multi-data set analysis of variability and change  
503 in Arctic spring snow cover extent, 1967-2008. *J. Geophys. Res.*, 115, D16111.

504

505 Bulygina, O.N., Razuvaev, V.N., Korshunova, N.N., 2009. Changes in snow cover over  
506 Northern Eurasia in the last few decades. *Environ. Res. Lett.*, 4, doi:10.1088/1748-  
507 9326/4/4/045026.

508

509 Cazenave, A., Remy, F., Dominh, K., Douville, H., 2000. Global ocean mass variation,  
510 continental hydrology and the mass balance of Antarctica ice sheet at seasonal time scale.  
511 *Geophys. Res. Lett.*, 27, 3755-3758.

512

513 Cazenave, A., Llovel, W., 2010. Contemporary sea level rise. *Annu. Rev. Mar. Sci.*, 2, 145-  
514 173, doi:10.1146/annurev-marine-120308-081105.

515

516 Chang, A.T.C., Kelly, R.E.J., Josberger, E.G., Armstrong, R.L., Foster, J.L., Mognard, N.M.,  
517 2005. Analysis of ground-measured and passive microwave derived snow depth variations in  
518 mid-winter across the Northern Great Plains. *J. Hydrometeorol.*, 6, 20-33.

519

520 Chen, F., Mitchell, K., Schaake, J., Xue, Y., Pan, H.-L., Koren, V., Duan, Q.Y., Ek, M., Betts,  
521 A., 1996. Modeling of land-surface evaporation by four schemes and comparison with FIFE  
522 observations. *J. Geophys. Res.*, 101, D3, 7251-7268.

523

524 Chen, J.L., Wilson, C.R., Chambers, D.P., Nerem, R.S., Tapley, B.D., 1998. Seasonal global  
525 water mass budget and mean sea level variations. *Geophys. Res. Lett.*, 25, 3555-3558.

526

527 Cohen, J., Barlow, M., Kushner, P.J., Saito, K., 2007. Stratosphere-Troposphere coupling and  
528 links with Eurasian land surface variability. *J. Clim.*, 20, 5335-5343.

529

530 Dee, D.P., Uppala, S., 2009. Variational bias correction of satellite radiance data in the ERA-  
531 interim reanalysis. *Q. J. R. Meteorol. Soc.*, 135, 1830-1841.

532

533 Derksen, C., Toose, P., Rees, A., Wang, L., English, M., Walker, A., Sturm, M., 2010.

534 Development of a tundra-specific snow water equivalent retrieval algorithm for satellite

535 passive microwave data. *Remote Sens. Environ.*, 114, 1699-1709.

536

537 Déry, S.J., Brown, R.D., 2007. Recent Northern Hemisphere snow cover extent trends and

538 implications for the snow-albedo feedback. *Geophys. Res. Lett.*, 34, L22504.

539

540 Dobson, A.J., 1990. An introduction to generalized linear models. CRC Press, New York.

541

542 Dyer, J.L., Mote, T.L., 2006. Spatial variability and trends in snow depth over North America.

543 *Geophys. Res. Lett.*, 33, L16503.

544

545 Enfield, D.B., Mestas-Nunez, A.M., Trimble, P.J., 2001. The Atlantic Multidecadal

546 Oscillation and its relationship to rainfall and river flows in the continental U.S.. *Geophys.*

547 *Res. Lett.*, 28, 2077-2080.

548

549 Foster, D.J., Davy, R.D., 1988. Global snow depth multi-year average. USAFETAC/TN-

550 88/006, Illinois: Scott Air Force Base, 48 pp.

551



552 Frappart, F., Ramillien, G., Biancamaria, S., Mognard, N.M., Cazenave, A., 2006. Evolution  
553 of high-latitude snow mass derived from the GRACE gravimetry mission (2002-2004).  
554 *Geophys. Res. Lett.*, 33, L02501.  
555  
556 Frappart, F., Ramillien, G., Famiglietti, J.S., in press. Water balance of the Arctic drainage  
557 system using GRACE gravimetry products. *Int. J. Remote Sens.*, doi:  
558 10.1080/01431160903474954.  
559  
560 Ghatak, D., Gong, G., Frei, A., 2010. North American temperature, snowfall, and snow-depth  
561 response to winter climate modes. *J. Clim.*, 23, 2320-2332.  
562  
563 Ge, Y., Gong, G., 2008. Observed inconsistencies between snow extent and snow depth  
564 variability at regional/continental scales. *J. Clim.*, 21, 1066-1082.  
565  
566 Ge, Y., Gong, G., 2009. North American snow depth and climate teleconnection patterns. *J.*  
567 *Clim.*, 22, 217-233.  
568  
569 Grippa, M., Mognard, N.M., Le Toan, T., Josberger, E.G., 2004. Siberia snow depth multi-  
570 year average derived from SSM/I data using a combined dynamic and static algorithm.  
571 *Remote Sens. Environ.*, 93, 30-41.  
572  
573 Grippa, M., Mognard, N.M., Le Toan, T., 2005. Comparison between the interannual  
574 variability of snow parameters derived from SSM/I and the Ob river discharge. *Remote Sens.*  
575 *Environ.*, 98, 35-44.  
576

577 Groisman, P.Y., Knight, R.W., Razuvaev, V.N., Bulygina, O.N., Karl, T.R., 2006. State of the  
578 ground: climatology and changes during the past 69 years over Northern Eurasia for a rarely  
579 used measure of snow cover and frozen land. *J. Clim.*, 19, 4933-4955.  
580

581 Guinehut, S., Coatanoan, C., Dhomps, A.-L., Le Traon, P.-Y., Larnicol, G., 2009. On the use  
582 of satellite altimeter data in Argo quality control. *J. Atmos. Oceanic Technol.*, 46, 85-98.  
583

584 Kalnay, E., Kanamitsu, M., Kistler, R., Collins, W., Deaven, D., Gandin, L., Iredell, M., Saha,  
585 S., White, G., Woollen, J., Zhu, Y., Chelliah, M., Ebisuzaki, W., Higgins, W., Janowiak, J.,  
586 Mo, K.C., Ropelewski, C., Wang, J., Leetmaa, A., Reynolds, R., Jenne, R., Joseph D., 1996.  
587 The NCEP/NCAR 40-year reanalysis project. *Bull. Am. Meteorol. Soc.*, 77, 437-471.  
588

589 Kaser, G., Cogley, J.G., Dyurgerov, M.B., Meier, M.F., Ohmura, A., 2006. Mass balance of  
590 glaciers and ice caps: Consensus estimates for 1961-2004. *Geophys. Res. Lett.*, 33, L19501.  
591

592 Kerr, R.A., 2000. A North Atlantic climate pacemaker for the centuries. *Science*, 288, 1984-  
593 1986.  
594

595 Kitaev, L., Førland, E., Razuvaev, V., Tveito, O.E., Krueger, O., 2005. Distribution of snow  
596 cover over Northern Eurasia. *Nord. Hydrol.*, 36, 311-319.  
597

598 Knight, J.R., Folland, C.K., Scaife, A.A., 2006. Climate impacts of the Atlantic Multidecadal  
599 Oscillation. *Geophys. Res. Lett.*, 33, L17706.  
600

601 Koster, R.D., Suarez, M. J., 1996. Energy and water balance calculations in the Mosaic LSM,  
602 NASA Tech. Memo. 104606, 9, 76 pp.  
603  
604 Liston, G.E., Sturm, M., 1998. Global Seasonal Snow Classification System. National Snow  
605 and Ice Data Center Digital media, Boulder, CO, USA.  
606  
607 Llovel, W., Guinehut, S., Cazenave, A., 2010. Regional and interannual variability in sea  
608 level over 2002-2009 based on satellite altimetry, Argo float data and GRACE ocean mass.  
609 Ocean Dynam., 60, 1193-1204, doi:10.1007/s10236-010-0324-0.  
610  
611 Mantua, N.J., Hare, S.R., Zhang, Y., Wallace, J.M., Francis, R.C., 1997. A Pacific  
612 interdecadal climate oscillation with impacts on salmon production. Bull. Am. Meteorol. Soc.,  
613 78, 1069-1079.  
614  
615 Milly, P.C.D., Cazenave, A., Gennero, M.-C., 2003. Contribution of climate-driven change in  
616 continental water storage to recent sea-level rise. Proc. Natl. Acad. Sci. U.S.A., 100, 13158-  
617 13161.  
618  
619 Minster, J.F., Cazenave, A., Serafini, Y.V., Mercier, F., Gennero, M.-C., Rogel, P., 1999.  
620 Annual cycle in mean sea level from Topex-Poseidon and ERS-1: inference on the global  
621 hydrological cycle. Global Planet. Change, 20, 57-66.  
622  
623 Mognard, N.M., Josberger, E.G., 2002. Northern Great Plains 1996/97 seasonal evolution of  
624 snowpack parameters from satellite passive-microwave measurements. Ann. Glaciol., 34, 15-  
625 23.

626

627 Orsolini, Y.J., Kvamstø, N.G., 2009. Role of Eurasian snow cover in wintertime circulation:  
628 Decadal simulations forced with satellite observations. *J. Geophys. Res.*, 114, D19108.

629

630 Paulson, A., Zhong, S., Wahr, J., 2007. Inference of mantle viscosity from GRACE and  
631 relative sea level data. *Geophys. J. Int.*, 171, 497-508.

632

633 Ramillien, G., Frappart, F., Cazenave, A., Güntner, A., 2005. Time variations of the land  
634 water storage from an inversion of 2 years of GRACE geoids. *Earth Planet. Sci. Lett.*, 235,  
635 283-301.

636

637 Rodell, M., Houser, P.R., Jambor, U., Gottschalck, J., Mitchell, K., Meng, C.-J., Arsenault,  
638 K., Cosgrove, B., Radakovich, J., Bosilovich, M., Entin, J.K., Walker, J.P., Lohmann, D.,  
639 Toll, D., 2004. The global land data assimilation system. *Bull. Am. Meteorol. Soc.*, 85, 381-  
640 394.

641

642 Sessa, R., Dolman, H., 2008. *Terrestrial Essential Climate Variables*, GTOS n°52, biennial  
643 report supplement, 40 pp., FAO, Rome, Italy.

644

645 Stocker, T.F., Raible, C.C., 2005. Water cycle shifts gear. *Nature*, 434, 830-833.

646

647 Thompson, D.W.J., Wallace, J.M., 1998. The Arctic Oscillation signature in the wintertime  
648 geopotential height and temperature fields. *Geophys. Res. Lett.*, 25, 1297-1300

649

650 Trenberth, K.E., Jones, P.D., Ambenje, P., Bojariu, R., Easterling, D., Klein Tank, A., Parker,  
651 D., Rahimzadeh, F., Renwick, J. A., Rusticucci, M., Soden, B., Zhai, P., 2007. Observations:  
652 Surface and Atmospheric Climate Change. In *Climate change 2007: the physical science*  
653 *basis. Contribution of Working Group I to the Fourth Assessment report of the*  
654 *Intergovernmental Panel on Climate Change*, edited by S. Solomon et al., pp. 235-336 and  
655 SM.3-8, Cambridge Univ. Press, Cambridge, U. K.

656

657 Uppala, S., Dee, D., Kobayashi, S., Berrisford, P., Simmons, A., 2008. Towards a climate  
658 data assimilation system: status update of ERA-Interim. *ECMWF newsletter*, 115, 12-18.

659

660 Wallace, J.M., Gutzler, D.S., 1981. Teleconnections in the geopotential height field during the  
661 Northern Hemisphere winter. *Mon. Wea. Rev.*, 109, 784-812.

662

663 Yang, D., Robinson, D., Zao, Y., Estilow, T., Ye, B., 2003. Streamflow response to seasonal  
664 snow cover extent changes in large Siberian watersheds. *J. Geophys. Res.*, 108, 4578, doi:  
665 10.1029/2002JD003419.

666 Table captions:

667

668 Table 1. Annual snow volume trends over 2003/2006 computed from SSM/I snow volume,  
669 snow reservoir extracted from GRACE and from the total GRACE signal over the whole  
670 study domain, Eurasia and North America

671

672 Table 2. Mean, standard deviation and trend of annual snow volume retrieved from SSM/I  
673 measurements during 1989/2006 period over the whole study domain, Eurasia and North  
674 America; p-values (p) for trends are indicated in parentheses.

675

676 Table 3. Correlation coefficients from January to March average of the climate indices (AO,  
677 AMO, PDO and PNA) and annual snow volumes over North America and Eurasia (the p-  
678 value of each correlation is indicated in parentheses). The correlations are computed both with  
679 and without trend in the time series of both snow volume and climate indices.

680

681

682 Figure captions:

683

684 Figure 1. Total snow volume for all continental surfaces above 50°N (Greenland excluded)  
685 estimated from SSM/I (red curve), GRACE (orange curve), ERA-interim reanalysis (black  
686 curve), MOSAIC model (green curve) and NOAH model (blue curve).

687

688 Figure 2. Annual snow volume from SSM/I data (solid red curve) over the whole study  
689 domain (a.), over Eurasia (b.) and over North America (c.). On each plot the black line  
690 corresponds to the linear trend and the blue curve corresponds to the linear combination of

691 two climate indices (January to March average) which best correlates with SSM/I snow  
692 volume (the mean value of the SSM/I snow volume over the 1989/2006 period has been  
693 added to the linear combination).

694

695 Figure 3. Map of the annual snow depth trends over the 1989/2006 time span. Only  
696 statistically significant trends are shown (i.e. trends with p-value < 0.1).

697

698 Figure 4. Annual snow volume over Eurasia (red curves in a., b., c., d.) and over North  
699 America (red curves in e., f., g., h.) and January to March average of AO (blue cruves in a.,  
700 e.), AMO (blue cruves in b., f.), PDO (blue cruves in c., g.) and PNA (blue cruves in d., h.)  
701 indices versus time. The time series have been normalized and centered to be plotted at the  
702 same scale. On each plot, the gray horizontal line corresponds to the zero in the original  
703 climate index time series.

704

705 Figure 5. Regression maps between annual snow volume and January to March average of  
706 AO (a.), AMO (b.), PDO (c.) and PNA (d.) indices for the 1989/2006 time span. On each map  
707 are shown pixels with a statistically significant (p-value < 0.1) correlation coefficient between  
708 snow volume and the considered climate index.

Tables:

Table 1:

Annual snow volume trend for 2003/2006 (km <sup>3</sup> .year <sup>-1</sup> )					
	SSM/I	GRACE snow no PGR corr.	PGR corr.	GRACE total no PGR corr.	PGR corr.
Whole domain	-71.4±83.5 (p=0.48)	46.8±103.4 (p=0.70)	-448.8	179.0±234.3 (p=0.52)	-316.6
Eurasia	-20.0±82.8 (p=0.83)	-91.3±57.5 (p=0.25)	-122.5	-237.2±231.4 (p=0.41)	-268.4
North America	-51.4±9.6 (p=0.03)	138.1±46.2 (p=0.10)	-326.3	416.3±52.0 (p=0.02)	-48.1

Table 2:

	SSM/I annual snow volume		
	Whole domain	Eurasia	North America
1989/2006 mean (km <sup>3</sup> )	3713	2272	1441
Std (km <sup>3</sup> )	218	189	95
Trend (km <sup>3</sup> .year <sup>-1</sup> )	1.5±10.5 (p=0.88)	11.3±9.3 (p=0.25)	-9.7±3.8 (p=0.02)

709  
710  
711  
712

Table 3 :

		AO	AMO	PDO	PNA
Eurasian snow depth	with trend	-0.57 (p=0.01)	0.04 (p=0.87)	0.49 (p=0.04)	0.30 (p=0.22)
	without trend	-0.51 (p=0.03)	-0.33 (p=0.18)	0.41 (p=0.09)	0.21 (p=0.39)
North American snow depth	with trend	0.51 (p=0.03)	-0.59 (p=0.01)	-0.18 (p=0.47)	-0.66 (p=0.003)
	without trend	0.25 (p=0.31)	-0.31 (p=0.20)	0.10 (p=0.71)	-0.58 (p=0.01)

713



714 Figures:

715

Figure 1:

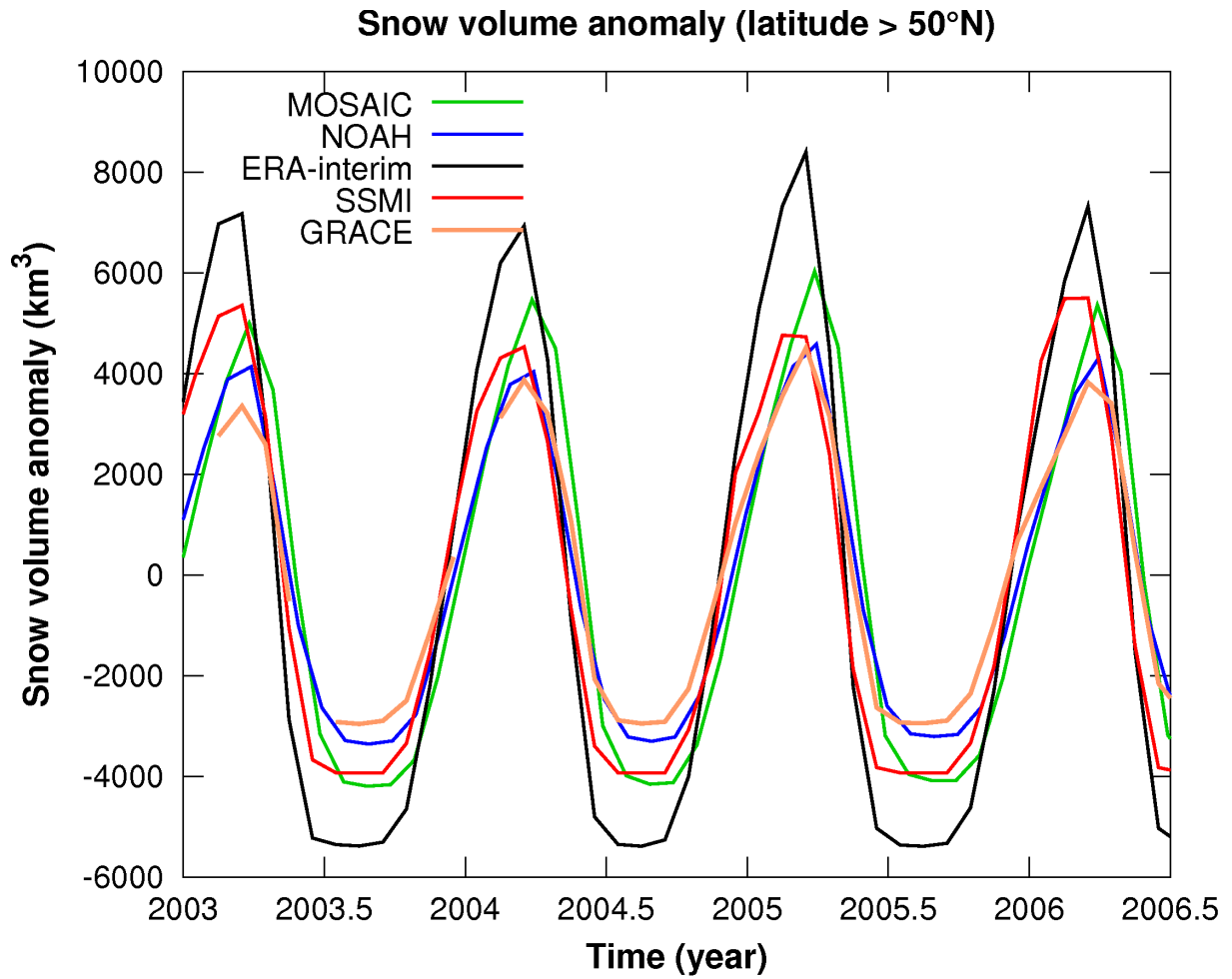


Figure 2:

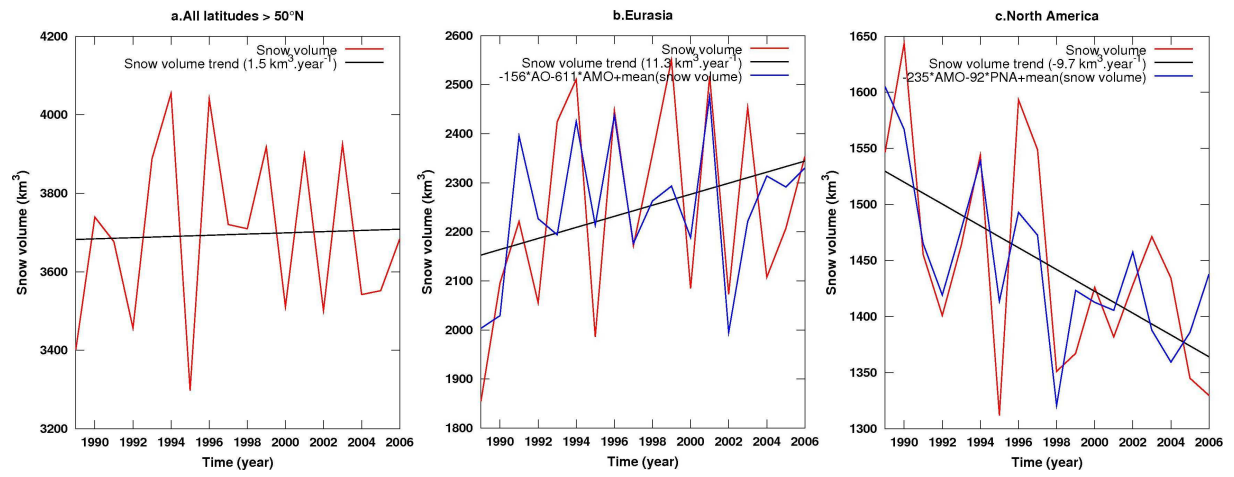


Figure 3:

### SSM/I snow depth trend (1989/2006)

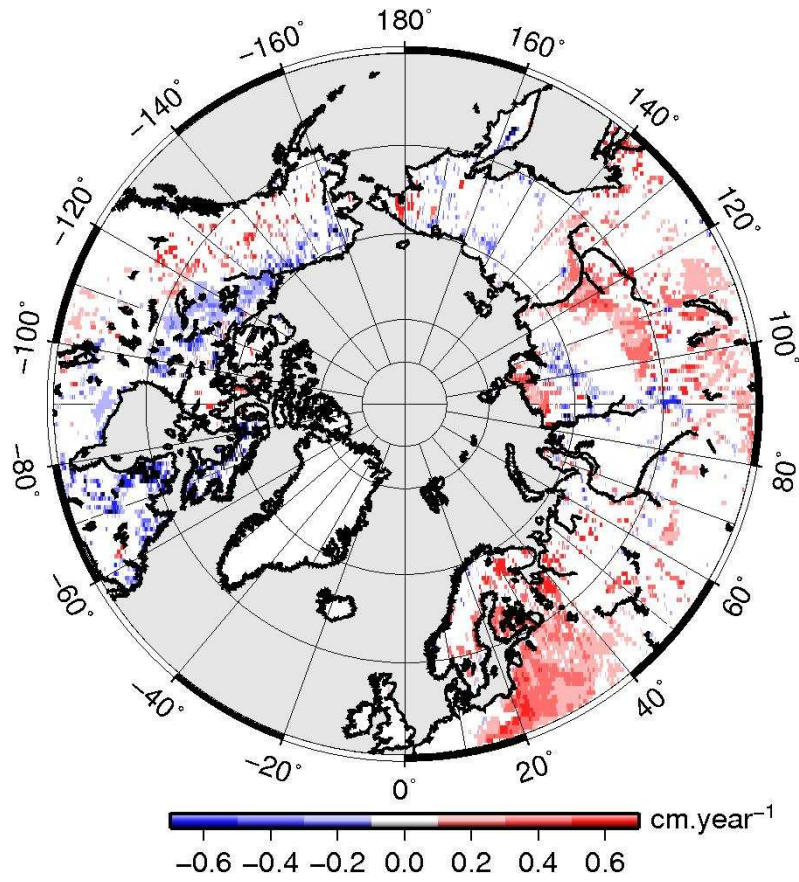


Figure 4 :

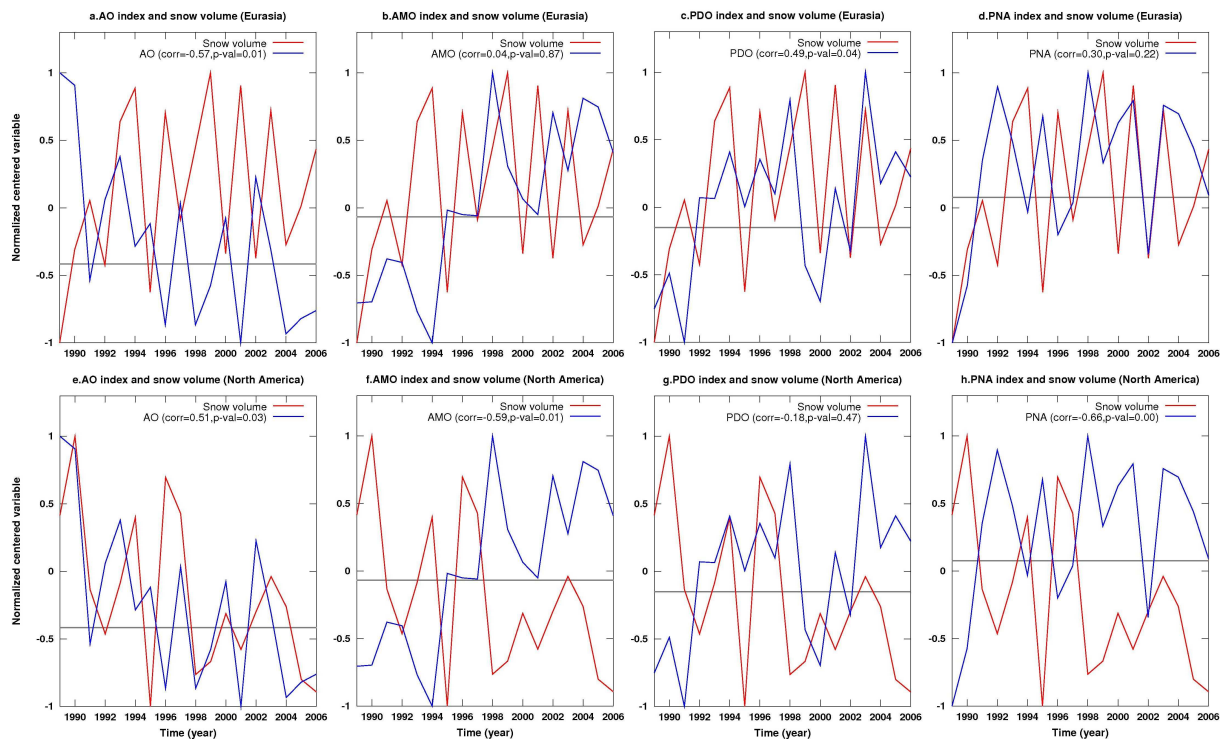
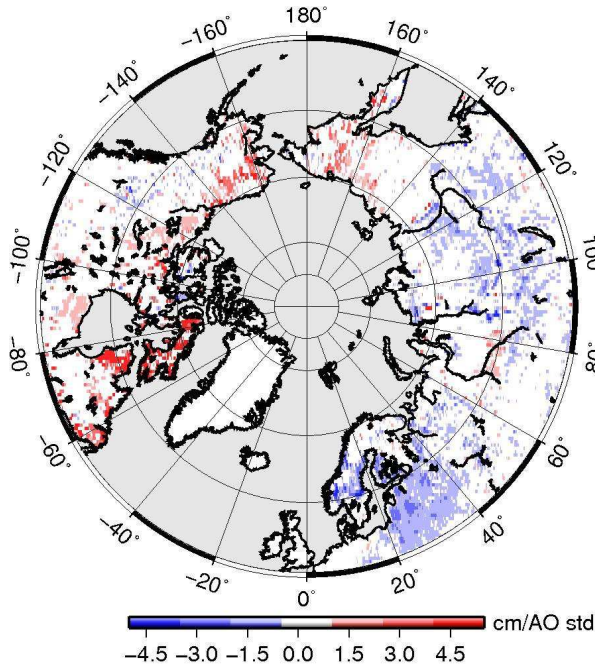
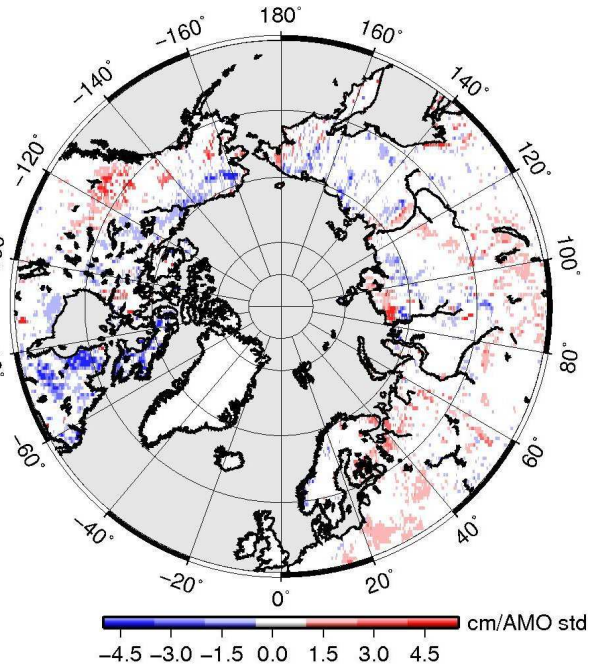


Figure 5:

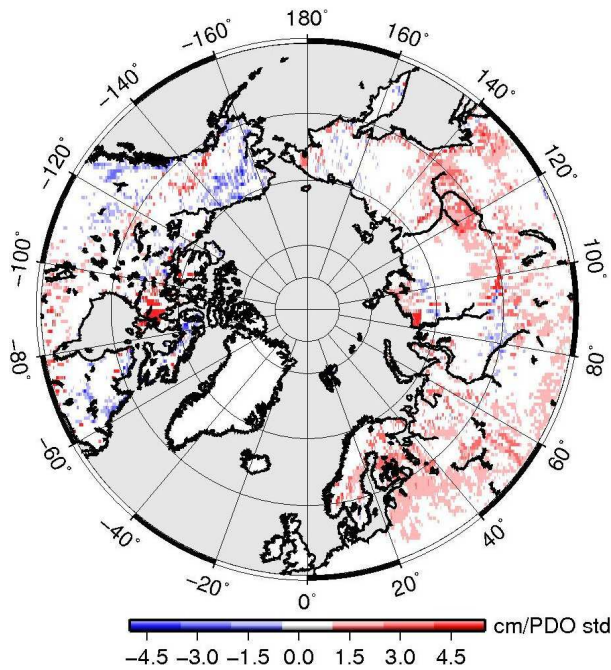
a. Regression map Snow Depth/AO



b. Regression map Snow Depth/AMO



c. Regression map Snow Depth/PDO



d. Regression map Snow Depth/PNA

